Binding of *meso*-Tetrakis(*N*-methylpyridinium-4-yl)porphyrin to Double Helical RNA and DNA·RNA Hybrids

Tadayuki Uno,* Kanya Hamasaki, Masahiko Tanigawa, and Saburo Shimabayashi

Faculty of Pharmaceutical Sciences, University of Tokushima, Shomachi, Tokushima 770, Japan

Received July 12, 1996[⊗]

The binding properties of *meso*-tetrakis(*N*-methylpyridinium-4-yl)porphyrin (H_2TMPyP) to RNA and DNA·RNA hybrid duplexes were studied by absorption and circular dichroism (CD) spectra. The duplexes studied were poly(rA)·poly(rU), poly(rA)·poly(dT), poly(rI)·poly(rC), poly(rI)·poly(dC), poly(rG)·poly(rC), and poly(rG)·poly(dC). The hypochromicity (about 40%) and the bathochromic shift (about 15 nm) of the porphyrin Soret absorption band upon binding were quite similar among the duplexes examined. The large bathochromic shift and hypochromicity suggested a significant perturbation in the porphyrin π electrons upon binding. H_2TMPyP was found to bind in a single step to poly(rI)·poly(rC), poly(rG)·poly(rC), and poly(rG)·poly(dC) and in a multistep manner to poly(rA)·poly(rU), poly(rA)·poly(dT), and poly(rI)·poly(dC). The induced CD spectra in the visible range suggested that the porphyrin preferred to bind to the RNA duplexes with self-stacking along the polymer surface and to the hybrids with intercalation, at least at higher duplex load. This implied a distinct conformational difference between the RNA duplexes and DNA·RNA hybrids, and a drug molecule is able to recognize the difference. The number of binding sites per base pairs (*n*), however, was very different among the RNA duplexes examined. We also found that the intensity of the bisignate-induced CD bands is proportional to the *n* value. This suggested that the transition moments on the neighboring porphyrins are interacting considerably with each other to produce intense induced CD peaks.

Introduction

The interactions of water-soluble, cationic porphyrins with DNA have been the subject of many recent investigations.[1−18] They have been excellent probes of nucleic acid structure and dynamics[19−22] since they provide intense chromophores and are monitored conveniently. The understanding of the interactions will lead porphyrins and their metal derivatives to medical applications to the inhibition of AIDS virus, HIV-1,[23,24] and photodynamic therapy of tumors.[25−28] The water-soluble porphyrins are readily derivatized, and some of them have been reported as showing nuclease activity.[11,29−32]

Three major modes have been proposed in the porphyrin binding to DNA:[20−22,33−36] intercalation, simple outside (external) binding, and outside binding with self-stacking along the DNA surface. Partial intercalation has also been suggested.[37,38]

[⊗] Abstract published in *Advance ACS Abstracts,* March 15, 1997.

(1) Gray, T. A.; Yue, K. T.; Marzilli, L. G. *J. Inorg. Biochem.* **1990**, *40*, 205−219.
(2) Yue, K. T.; Lin, M.; Gray, T. A.; Marzilli, L. G. *Inorg. Chem.* **1991**, *30*, 3214−3222.
(3) Feng, Y.; Pilbrow, J. R. *Biophys. Chem.* **1990**, *36*, 117−131.
(4) Kuroda, R.; Takahashi, E.; Austin, C. A.; Fisher, L. M. *FEBS Lett.* **1990**, *262*, 293−298.
(5) Sari, M. A.; Battioni, J. P.; Dupre, D.; Mansuy, D.; Le Pecq, J. B. *Biochemistry* **1990**, *29*, 4205−4215.
(6) Slama-Schwok, A.; Lehn, J.-M. *Biochemistry* **1990**, *29*, 7895−7903.
(7) Mukundan, N. E.; Petho, G.; Dixon, D. W.; Kim, M. S.; Marzilli, L. G. *Inorg. Chem.* **1994**, *33*, 4676−4687.
(8) Pasternack, R. F.; Bustamante, C.; Collings, P. J.; Giannetto, A.; Gibbs, E. J. *J. Am. Chem. Soc.* **1993**, *115*, 5393−5399.
(9) Mukundan, N. E.; Petho, G.; Dixon, D. W.; Marzilli, L. G. *Inorg. Chem.* **1995**, *34*, 3677−3687.
(10) Lin, M.; Lee, M.; Yue, K. T.; Marzilli, L. G. *Inorg. Chem.* **1993**, *32*, 3217−3226.
(11) Ding, L.; Etemad-Moghadam, G.; Meunier, B. *Biochemistry* **1990**, *29*, 7868−7875.
(12) Hudson, B. P.; Sou, J.; Berger, D. J.; McMillin, D. R. *J. Am. Chem. Soc.* **1992**, *114*, 8997−9002.
(13) Yue, K. T.; Lin, M.; Gray, T. A.; Marzilli, L. G. *Inorg. Chem.* **1991**, *30*, 3214−3222.
(14) Kuroda, R.; Tanaka, H. *J. Chem. Soc., Chem. Commun.* **1994**, 1575−1576.
(15) Pasternack, R. F.; Brigandi, R. A.; Abrams, M. J.; Williams, A. P.; Gibbs, E. J. *Inorg. Chem.* **1990**, *29*, 4483−4486.
(16) Pasternack, R. F.; Giannetto, A.; Pagano, P. Gibbs, E. J. *J. Am. Chem. Soc.* **1991**, *113*, 7799−7800.
(17) Marzilli, L. G.; Petho, G.; Lin, M.; Kim, M. S.; Dixon, D. W. *J. Am. Chem. Soc.* **1992**, *114*, 7575−7577.
(18) Petho, G.; Elliott, N. B.; Kim, M. S.; Lin, M.; Dixon, D. W.; Marzilli, L. G. *J. Chem. Soc., Chem. Commun.* **1993**, 1547−1548.
(19) Pasternack, R. F.; Gibbs, E. J.; Villafranca, J. J. *Biochemistry* **1983**, *22*, 5409−5417.
(20) Pasternack, R. F.; Gibbs, E. J. *ACS Symp. Ser.* **1989**, No. *402*, 59−73.
(21) Fiel, R. J. *J. Biomol. Struct. Dyn.* **1989**, *6*, 1259−1274.
(22) Marzilli, L. G. *New J. Chem.* **1990**, *14*, 409−420.
(23) Dixon, D. W.; Marzilli, L. G.; Schinazi, R. *Ann. N.Y. Acad. Sci.* **1990**, *616*, 511−513.
(24) Sessler, J. L.; Cyr, M. J.; Lynch, V. *J. Am. Chem. Soc.* **1990**, *112*, 2810−2813.
(25) Musser, D. A.; Datta-Gupta, N.; Fiel, R. J. *Biochem. Biophys. Res. Commun.* **1980**, *97*, 918−925.
(26) Fiel, R. J.; Datta-Gupta, N.; Mark, E. H.; Howard, J. C. *Cancer Res.* **1981**, *41*, 3543−3545.
(27) Praseuth, D.; Gaudemer, A.; Verlhac, J.-B.; Kraljic, I.; Sissoeff, I.; Guille, E. *Photochem. Photobiol.* **1986**, *44*, 717−724.
(28) Villaneuva, A.; Hazen, M. J.; Stockert, J. C. *Experientia* **1986**, *42*, 1269−1271.
(29) Fiel, R. J.; Beerman, T. A.; Mark, E. H.; Datta-Gupta, N. *Biochem. Biophys. Res. Commun.* **1982**, *107*, 1067−1074.
(30) Dabrowiak, J. C.; Ward, B.; Goodisman, J. *Biochemistry* **1989**, *28*, 3314−3322.
(31) Bernadou, J.; Pratviel, G.; Bennis, F.; Girardet, M.; Meunier, B. *Biochemistry* **1989**, *28*, 7268−7275.
(32) Pitie, M.; Pratviel, G.; Bernadou, J.; Meunier, B. *Proc. Natl. Acad. Sci. U.S.A.* **1992**, *89*, 3967−3971.
(33) Carvlin, M. J.; Fiel, R. J. *Nucleic Acids Res.* **1983**, *11*, 6121−6139.
(34) Carvlin, M. J.; Mark, E.; Fiel, R. J. *Nucleic Acids Res.* **1983**, *11*, 6141−6154.
(35) Banville, D. L.; Marzilli, L. G.; Strickland, J. A.; Wilson, W. D. *Biopolymers* **1986**, *25*, 1837−1858.
(36) Strickland, J. A.; Banville, D. L.; Wilson, W. D.; Marzilli, L. G. *Inorg. Chem.* **1987**, *26*, 3398−3406.
(37) Ford, K. G.; Pearl, L. H.; Neidle, S. *Nucleic Acids Res.* **1987**, *15*, 6553−6562.
(38) Dougherty, G. *J. Inorg. Biochem.* **1988**, *34*, 95−103.

S0020-1669(96)00824-5 CCC: $14.00

The binding mode is highly dependent on the substituent groups of the porphyrin, metal center, the type of DNA, and the ionic strength of the medium.[20−22] In order to achieve intercalation, it has been proposed that the porphyrin must have a limited effective thickness.[19,33,39] When nonplanar *N*-trimethylammonium substituents were attached, or Fe(III), Co(III), Mn(III), or Zn(II) which binds axial ligands was inserted, the porphyrin becomes an outside binder. The porphyrins intercalate in regions of DNA with a high percentage of GC base pairs, presumably at 5′-CG sites,[40,41] and undergo outside binding in regions of high AT base pairs.[10,21,22] The increase of ionic strength occasionally promotes long-range aggregates on the nucleic acid polymer, resulting in a helical alignment of porphyrin on the surface of the polymer.[8,16,21,33−36,42,43]

Various spectroscopic techniques, such as NMR,[35,40,41,44] circular dichroism (CD),[33,34,39,45,46] fluorescence,[5,47] electron spin resonance,[48] UV−visible absorption,[19,29,33,34,44−46] and resonance Raman spectroscopy,[49−55] were applied to a multitude of different DNA polymers, and the binding modes have been distinguished. The sign of the induced CD spectrum of porphyrins bound to nucleic acids provides conveniently a signature for the binding mode to DNA:[14,46,56] a positive induced CD band in the Soret region is indicative of external (minor) groove binding, and a negative induced CD band is present upon intercalation. Some of the porphyrins produce intense bisignate CD spectra whose profiles reveal the helical sense of the DNA. The helical alignment of porphyrin transition dipoles gives rise to the very large, conservative CD signals observed.[15,16,43]

In spite of the extensive studies on the interactions of water-soluble porphyrins with DNA, the binding properties for neither RNA duplex nor DNA·RNA hybrid have been examined thus far. The DNA·RNA hybrids were recently shown[57] to have higher affinity to Zn finger proteins than DNA. This may suggest that the porphyrins should have distinct binding properties to the hybrids relative to DNA duplexes. Here we report the interaction of water-soluble cationic porphyrin, *meso*-tetrakis(*N*-methylpyridinium-4-yl)porphyrin (H_2TMPyP), with six homopolymer duplexes, poly(rA)·poly(rU), poly(rI)·poly(rC), poly(rG)·poly(rC) (RNA duplexes), poly(rA)·poly(dT), poly(rI)·poly(dC), and poly(rG)·poly(dC) (DNA·RNA hybrids). The GC and IC base pairs have similar hydrogen bonding, except for their having three and two hydrogen bondings, respectively (Figure 1). In this context, the IC base pair resembles AT and AU base pairs. Therefore, we may expect that we can depict a general feature for the binding of the porphyrin to RNA duplexes and DNA·RNA hybrids. This is the first report on the interactions of water-soluble porphyrin with RNA and DNA·RNA duplexes.

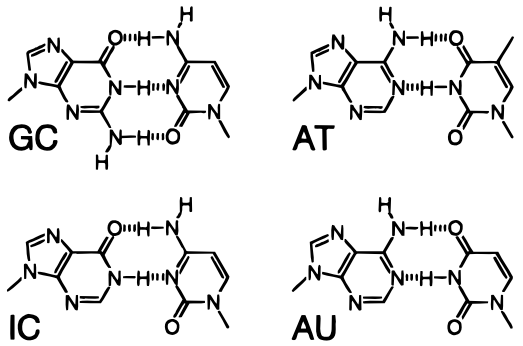

Figure 1. Base-pairing scheme.

Experimental Section

Materials. The tosylate salt of H_2TMPyP was purchased from Dojin Chemical Co. and dissolved in doubly distilled water. The stock solution was passed through a 0.45-μm filter, and the concentration of the porphyrin was determined from the extinction coefficient (226 mM^{-1} cm^{-1}) at 422 nm.[58] The single-strand homopolymers poly(rA), poly(rU), and poly(dT) were purchased from Sigma Chemical Co, while poly(rG), poly(rI), poly(rC), and poly(dC) were from Pharmacia. The nucleotide concentrations were determined from the appropriate molar absorptivity: 9.8 mM^{-1} cm^{-1} at 258 nm for poly(rA);[59] 9.35 mM^{-1} cm^{-1} at 260 nm for poly(rU);[59] 8.52 mM^{-1} cm^{-1} at 264 nm for poly(dT);[60] 10.4 mM^{-1} cm^{-1} at 253 nm for poly(rG);[59] 10.2 mM^{-1} cm^{-1} at 248 nm for poly(rI);[59] 6.2 mM^{-1} cm^{-1} at 269 nm for poly(rC);[59] and 6.8 mM^{-1} cm^{-1} at 274 nm for poly(dC).[59] The duplexes were prepared in solutions containing 10 mM sodium phosphate, 1 mM EDTA, and 0.1 M sodium chloride (pH 7.0) by mixing proper single strands in a 1:1 molar ratio. This solution was heated to 95 °C for 10 min and then cooled slowly to room temperature to minimize formation of competing secondary structures. The concentrations of the duplexes were expressed in terms of base pairs.

Spectral Measurements. Aliquots of a duplex solution to the solution of H_2TMPyP (4.96 μM) were added, and the absorption spectra were recorded with a Shimadzu UV-2100 spectrophotometer. The induced CD spectra of H_2TMPyP (4.96 μM) were measured with selected concentrations of the duplexes, and 20 independent spectra were averaged. In the case of poly(rG)·poly(rC), the induced signal was so weak that the porphyrin concentration was raised to 9.91 μM with averaging of 40 independent spectra. Conversely, to a solution of the duplexes (about 40 μM) was added aliquots of the H_2TMPyP solution, and four independent CD spectra in the UV range were averaged. The CD spectra were recorded with a Jasco J-600 spectropolarimeter, and all the spectra were base line corrected and smoothed. All the spectral measurements were made in a buffer containing 10 mM sodium phosphate, 1 mM EDTA, and 0.1 M sodium chloride (pH 7.0). The binding constants (*K*) and the number of binding

(39) Carvlin, M. J.; Datta-Gupta, N.; Fiel, R. J. *Biochem. Biophys. Res. Commun.* **1982**, *108*, 66−73.
(40) Banville, D. L.; Marzilli, L. G.; Wilson, W. D. *Biochem. Biophys. Res. Commun.* **1983**, *113*, 148−154.
(41) Marzilli, L. G.; Banville, D. L.; Zon, G.; Wison, W. D. *J. Am .Chem. Soc.* **1986**, *108*, 4188−4192.
(42) Pasternack, R. F.; Gibbs, E. J. *J. Organomet. Polym.* **1993**, *3*, 77−88.
(43) Gibbs, E. J.; Tinoco, I., Jr.; Maestre, M. F.; Ellinas, P. A.; Pasternack, R. F. *Biochem. Biophys. Res. Commun.* **1988**, *157*, 350−358.
(44) Pasternack, R. F.; Gibbs, E. S.; Gaudemer, A.; Antebi, A.; Bassner, S.; DePoy, L.; Turner, D. H.; Williams, A. Laplace, F.; Lamsurd, M. H.; Merienne, C.; Perree-Favet, M. *J. Am. Chem. Soc.* **1985**, *107*, 8179−8186.
(45) Fiel, R. J.; Howard, J. C.; Mark, E. H.; Datta-Gupta, N. *Nucleic Acids Res.* **1979**, *6*, 3093−3118.
(46) Pasternack. R. F.; Gibbs, E. J.; Villafranca, J. J. *Biochemistry* **1983**, *22*, 2406−2414.
(47) Kelly, J. M.; Murphy, M. J.; McConnel, D. J.; OhUigin, C. *Nucleic Acids Res.* **1985**, *13*, 167−184.
(48) Dougherty, G.; Pilbrow, J. R.; Skorobogaty, A.; Smith, T. D. *J. Chem. Soc., Faraday Trans. 2* **1985**, *81*, 1739−1759.
(49) Blom, N.; Odo, J.; Nakamoto, K.; Strommen, D. P. *J. Phys. Chem.* **1986**, *90*, 2847−2852.
(50) Butje, K.; Nakamoto, K. *Inorg. Chim. Acta* **1990**, *167*, 97−108.
(51) Butje, K.; Nakamoto, K. *J. Inorg. Biochem.* **1990**, *39*, 75−92.
(52) Butje, K.; Schneider, J. H.; Kim, J.-J. P.; Wang, Y.; Ikuta, S.; Nakamoto, K. *J. Inorg. Biochem.* **1989**, *37*, 119−134.
(53) Schneider, J. H.; Odo, J.; Nakamoto, K. *Nucleic Acids Res.* **1988**, *16*, 10323−10338.
(54) Turpin, P. Y.; Chinsky, L.; Laigle, A.; Tsuboi, M.; Kincaid, J. R.; Nakamoto, K. *Photochem. Photobiol.* **1990**, *51*, 519−525.
(55) Nonaka, Y.; Lu, D. S.; Dwivedi, A.; Strommen, D. P.; Nakamoto, K. *Biopolymers* **1990**, *29*, 999−1004.
(56) Pasternack, R. F.; Garrity, P.; Ehrlich, B.; Davis, C. B.; Gibbs, E. J.; Orloff, G.; Giartosio, A.; Turano, C. *Nucleic Acids Res.* **1986**, *14*, 5919−5931.
(57) Shi, Y.; Berg, J. M. *Science* **1995**, *268*, 282−284.
(58) Pasternack, R. F.; Huber, P. R.; Boyd, P.; Engasser, G.; Francesconi, L.; Gibbs, E.; Fasella, P.; Venturo, G. C. Hinds, L. C. *J. Am. Chem. Soc.* **1972**, *94*, 4511−4517.
(59) *The World of Pharmacia Biotech '95 '96*; Uppsala, 1995; p 283.
(60) Ts'o, P. O. P.; Rapaport, S. A.; Bollum, F. J. *Biochemistry* **1966**, *5*, 4153−4170.

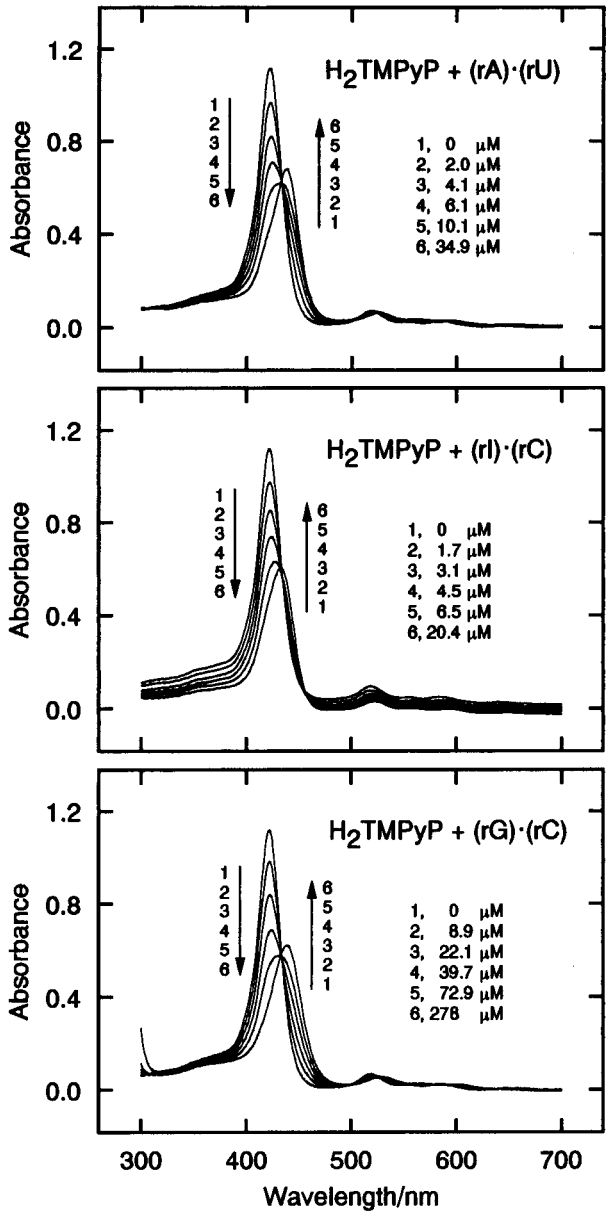

Figure 2. Absorption spectral change of H_2TMPyP on the addition of RNA duplexes. The porphyrin concentration was 4.96 μM. The spectra were recorded in 10 mM sodium phosphate, 1 mM EDTA, 0.1 M NaCl (pH 7.0). Top, concentrations of poly(rA)·poly(rU) were as follows: 1, 0; 2, 2.0; 3, 4.1; 4, 6.1; 5, 10.1; 6, 34.9 μM. Middle, concentrations of poly(rI)·poly(rC) were as follows: 1, 0; 2, 1.7; 3, 3.1; 4, 4.5; 5, 6.5; 6, 20.4 μM. Bottom, concentrations of poly(rG)·poly(rC) were as follows: 1, 0; 2, 8.9; 3, 22.1; 4, 39.7; 5, 72.9; 6, 278 μM.

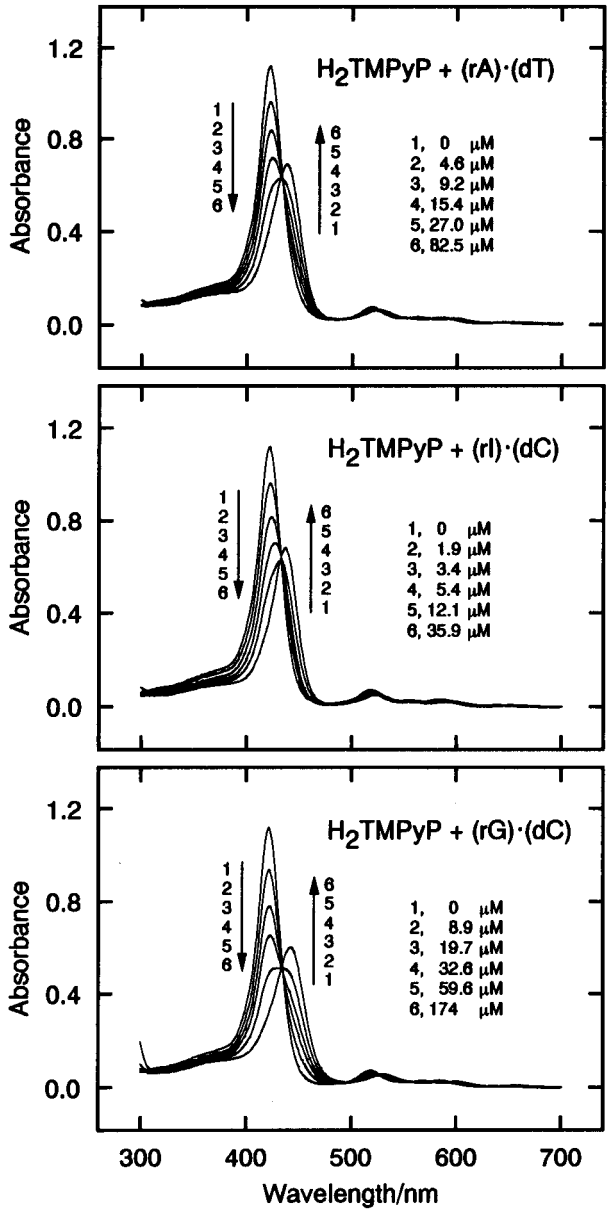

Figure 3. Absorption spectral change of H_2TMPyP on the addition of DNA·RNA hybrids. The porphyrin concentration was 4.96 μM. The spectra were recorded in 10 mM sodium phosphate, 1 mM EDTA, 0.1 M NaCl (pH 7.0). Top, concentrations of poly(rA)·poly(dT) were as follows: 1, 0; 2, 4.6; 3, 9.2; 4, 15.4; 5, 27.0; 6, 82.5 μM. Middle, concentrations of poly(rI)·poly(dC) were as follows: 1, 0; 2, 1.9; 3, 3.4; 4, 5.4; 5, 12.1; 6, 35.9 μM. Bottom, concentrations of poly(rG)·poly(dC) were as follows: 1, 0; 2, 8.9; 3, 19.7; 4, 32.6; 5, 59.6; 6, 174 μM.

sites per base pair (n) were estimated from the spectral changes, following the Scatchard analysis.[61−63]

Results

Absorption Spectra. In Figure 2 is shown the change in the absorption spectrum of H_2TMPyP with the addition of RNA duplexes. One set of isosbestic points was observed in each case, and the binding was found to proceed apparently in a single step. The Soret maximum shifted commonly to a longer wavelength (about 15 nm) and showed a large hypochromicity (about 40%). In Figure 3 is shown the absorption spectral change with the addition of DNA·RNA hybrids. The spectral change was quite similar to the RNA duplexes in both bathochromic shift and hypochromicity. A distinct set of isosbestic points was observed again, and hence the binding process was revealed to be a single step. The values for the hypochromicity and the bathochromic shift are summarized in Table 1. The large values for these parameters suggest that the porphyrin π electrons were perturbed considerably upon binding to the duplexes.

The absorbance changes at the Soret maximum against the concentration of base pairs are shown in Figure 4. It is clear that the porphyrin binding to poly(rI)·poly(dC) was a two-step process, although other duplexes showed a single binding step. As shown in Figure 3 (middle), isosbestic points were apparent that the two porphyrin species produced upon binding to the poly(rI)·poly(dC) must show quite similar absorption spectra,

(61) Scatchard, G. *Ann. N.Y. Acad. Sci.* **1949**, *51*, 660−672.
(62) McGhee, J. D.; von Hippel, P. H. *J. Mol. Biol.* **1974**, *86*, 469−489.
(63) Correia, J. J.; Chaires, J. B. *Methods Enzymol.* **1994**, *240*, 593−614.

Table 1. Spectroscopic Data for H_2TMPyP Bound to the Duplexes

duplexes	$\Delta\lambda$/nm[a]	H/%[b]	induced CD/nm[c]	
poly(rA)·poly(rU)	+16	39	441 (−4.7)	423 (+1.9)
poly(rI)·poly(rC)	+11	46	444 (−9.3)	421 (+5.0)
poly(rG)·poly(rC)	+17	44	443 (−0.5)	423 (+0.6)
poly(rA)·poly(dT)	+16	38	439 (−5.5)	
poly(rI)·poly(dC)	+15	39	439 (−6.1)	
			443 (−20.4)	423 (+8.8)
poly(rG)·poly(dC)	+20	46	442 (−4.6)	
poly(dA-dT)$_2$[d]	+7	7	433	
poly(dG-dC)$_2$[d]	+21	41	448	

[a] Bathochromic shift. [b] The hypochromicity (H/%) was determined by the equation $H = (\epsilon_f - \epsilon_b)/\epsilon_f \times 100$, where ϵ_f and ϵ_b represent the molar absorptivities of free and bound porphyrins, respectively, which were determined at the respective Soret maxima. [c] Induced CD peaks. The values in parentheses are molar ellipticities ($[\theta]/10^4$ deg cm^2 dmol^{-1}). [d] From ref 46.

and hence, the electronic structure of the two products must be nearly the same. For other duplexes, the binding process could be analyzed by a simple equilibrium reaction, and the binding constant (K) and the number of binding sites on the duplex per base pairs (n_{AB}) could be determined from the absorbance changes. The values of K and n_{AB} thus obtained are summarized in Table 2. Theoretical curves with these values were drawn in Figure 4 and were found to fit nicely to the absorbance changes actually observed. It is clear that the K values are commonly about 0.7 μM^{-1} except for poly(rI)·poly(rC), whereas the n_{AB} values scatter considerably. In the case of poly(rI)·poly(dC), the binding process was complex and the Scatchard analysis was not possible. In turn, the number of binding sites was estimated from the break points shown with arrows (Figure 4) to be 0.25 and 0.82.

CD Spectra. The absorbance changes mentioned above were traced by adding aliquots of duplex solutions to H_2TMPyP, and hence, the porphyrin exists in large excess at least at the initial stage. If the second (or third) binding step existed and the absorbance change was small, however, we might fail to detect this step. On the contrary, the undetected step(s), if present, could be revealed by CD spectral changes in the UV region, since the duplexes are now in large excess to the porphyrin at the initial stage. In addition, the CD spectra in the UV range is sensitive to the conformational change of the duplexes and, hence, would bring about different kinds of information on the binding.

In Figure 5 (top), the CD changes of the RNA duplexes are shown. In the case of poly(rA)·poly(rU), an isoelliptic point was seen at about 260 nm at the concentration of H_2TMPyP below 10 μM, and the CD spectral change was small. The spectrum, however, further changed greatly by the addition of H_2TMPyP, indicating that at least two binding processes exist and that drastic conformational change of the duplex occurred upon the addition of the porphyrin. The spectral change for poly(rI)·poly(rC) was also drastic, with an isoelliptic point at about 255 nm. The spectrum of poly(rG)·poly(rC) changed only slightly, and hence, the conformation of this duplex was almost unaffected by the binding of the porphyrin. In Figure 6 are shown the CD spectral changes of hybrid duplexes. One set of isoelliptic points is apparent in each case, although it was blurred for poly(rA)·poly(dT) upon addition of the porphyrin above 10 μM. In the case of poly(rG)·poly(dC), the two positive peaks at about 275 and 250 nm seem to be fused to give a stronger positive peak at 270 nm.

The changes of the ellipticity were plotted against the concentration of H_2TMPyP (Figure 7). The solid lines were drawn theoretically with the K and n_{AB} values obtained from

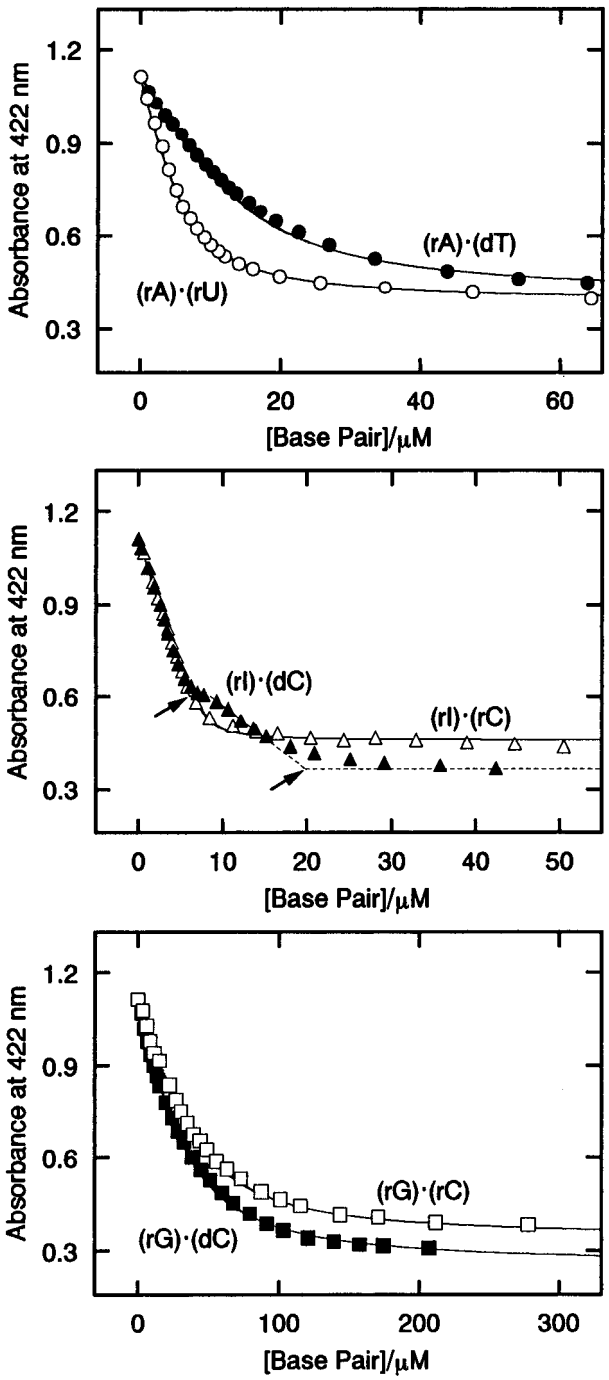

Figure 4. Absorbance change of H_2TMPyP at 422 nm by the addition of duplexes: Open circles, poly(rA)·poly(rU); closed circles, poly(rA)·poly(dT); open triangles, poly(rI)·poly(rC); closed triangles, poly(rI)·poly(dC); open squares, poly(rG)·poly(rC); closed squares, poly(rG)·poly(dC). Theoretical solid lines were drawn with the K and n_{AB} values in Table 2. Arrows indicate break points for the dashed line, which was drawn with the linear part of the absorbance change.

the absorbance change (Table 2). The theoretical curves for poly(rI)·poly(rC), poly(rG)·poly(rC), and poly(rG)·poly(dC) were in good accordance with the observed elliptic changes. This indicates that the binding proceeded in a single step, and both the absorbance and CD changes could trace the same binding process in the respective duplexes. In the case of poly(rA)·poly(rU) and poly(rA)·poly(dT), however, the observed elliptic changes deviated considerably from the theoretical curves (Figure 7), and hence, the CD changes could trace other binding steps which could not be detected by the absorbance changes (Figure 4). When two binding steps are distinct and can be treated separately, two n values are obtained indepen-

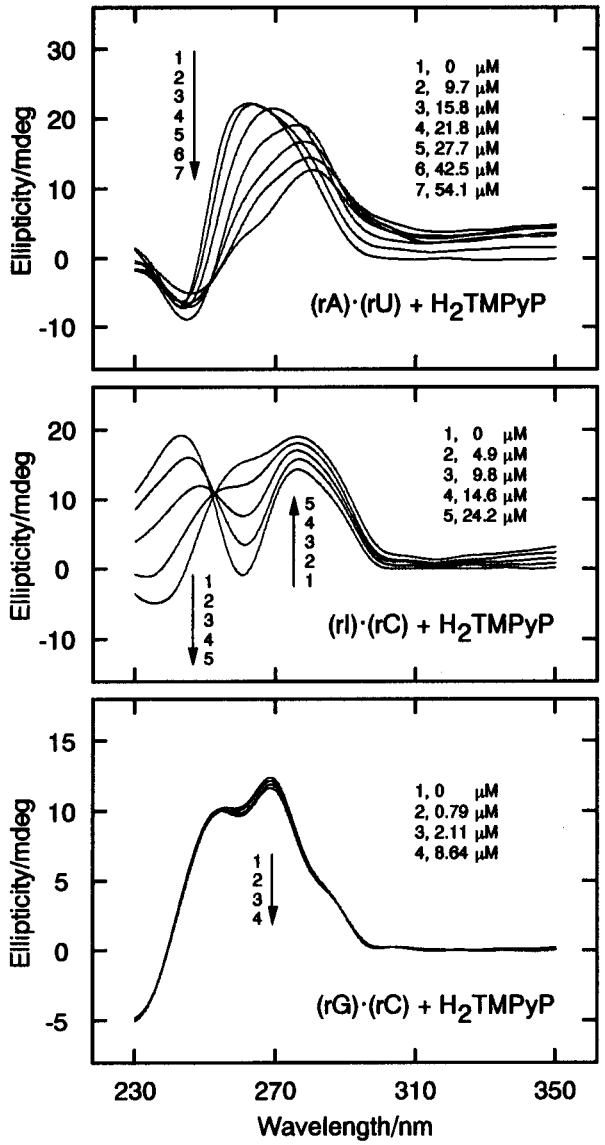

Figure 5. CD spectral changes of RNA duplexes upon addition of H_2TMPyP. The spectra were recorded in 10 mM sodium phosphate, 1 mM EDTA, 0.1 M NaCl (pH 7.0). Top: 38.5 μM poly(rA)·poly(rU). The concentrations of H_2TMPyP were as follows: 1, 0; 2, 9.7; 3, 15.8; 4, 21.8; 5, 27.7; 6, 42.5; 7, 54.1 μM. Middle: 38.9 μM poly(rI)·poly(rC). The concentrations of H_2TMPyP were as follows: 1, 0; 2, 4.9; 3, 9.8; 4, 14.6; 5, 24.2 μM. Bottom: 38.9 μM poly(rG)·poly(rC). The concentrations of H_2TMPyP were as follows: 1, 0; 2, 0.79; 3, 2.11; 4, 8.64 μM.

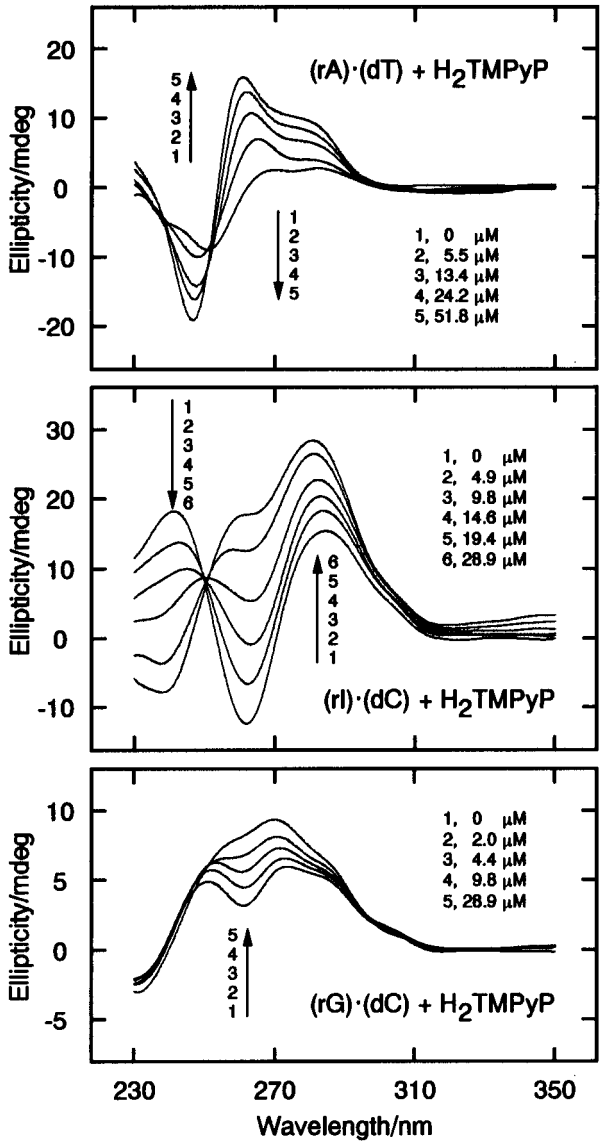

Figure 6. CD spectral changes of DNA·RNA hybrids upon addition of H_2TMPyP. The spectra were recorded in 10 mM sodium phosphate, 1 mM EDTA, 0.1 M NaCl (pH 7.0). Top: 38.5 μM poly(rA)·poly(dT). The concentrations of H_2TMPyP were as follows: 1, 0; 2, 5.5; 3, 13.4; 4, 24.2; 5, 51.8 μM. Middle: 38.9 μM poly(rI)·poly(dC). The concentrations of H_2TMPyP were as follows: 1, 0; 2, 4.9; 3, 9.8; 4, 14.6; 5, 19.4; 6, 28.9 μM. Bottom: 38.5 μM poly(rG)·poly(dC). The concentrations of H_2TMPyP were as follows: 1, 0; 2, 2.0; 3, 4.4; 4, 9.8; 5, 28.9 μM.

dently from the break points (shown by arrows) of the dashed lines in Figure 7. The n values (n_{CD}) were estimated and summarized in Table 2.

In the case of poly(rA)·poly(rU), two n values were obtained. The larger one ($n_{CD} = 0.82$) was quite similar to that obtained from the absorbance change ($n_{AB} = 0.79$). In the case of poly(rA)·poly(dT), on the contrary, the smaller one ($n_{CD} = 0.29$) was similar to that obtained from the absorbance change ($n_{AB} = 0.32$). Therefore, the $n = 0.3$ step for poly(rA)·poly(rU) and the $n = 0.7$ step for poly(rA)·poly(dT) were sensitive only to the conformational change of the duplexes. In the case of poly(rI)·poly(dC), the K and n_{AB} values could not be determined from the absorbance change that the number of binding sites (n_{CD}) was evaluated from the break point of the elliptic change (shown with an arrow in Figure 7). The value ($n_{CD} = 0.59$) coincided with neither of the n_{AB} values obtained from the absorbance changes (Table 2) such that the conformational change of poly(rI)·poly(dC) was not reflected directly on the electronic structure of the porphyrin.

Induced CD Spectra. To clarify the binding modes of the porphyrin, the induced CD spectra were measured at selected concentrations of the duplexes. We had to average 20 or 40 independent spectra to improve the spectral feature for every duplex. As seen in Figure 8, conservative-type CD peaks were observed commonly for RNA duplexes (upper three panels), and the porphyrin was suggested to bind externally with self-stacking along the polymer surface. In the case of poly(rA)·poly(rU), two-step binding was revealed by the elliptic change (Figure 7), but the negative peak only diminished slightly with the low duplex load corresponding to $n = 0.8$ step. It may suggest that the self-stacked porphyrin still dominated in the $n = 0.8$ step.

For the DNA·RNA hybrids, on the other hand, a negative CD band at about 440 nm was induced upon binding (lower three panels in Figure 8), and the intercalation was suggested.

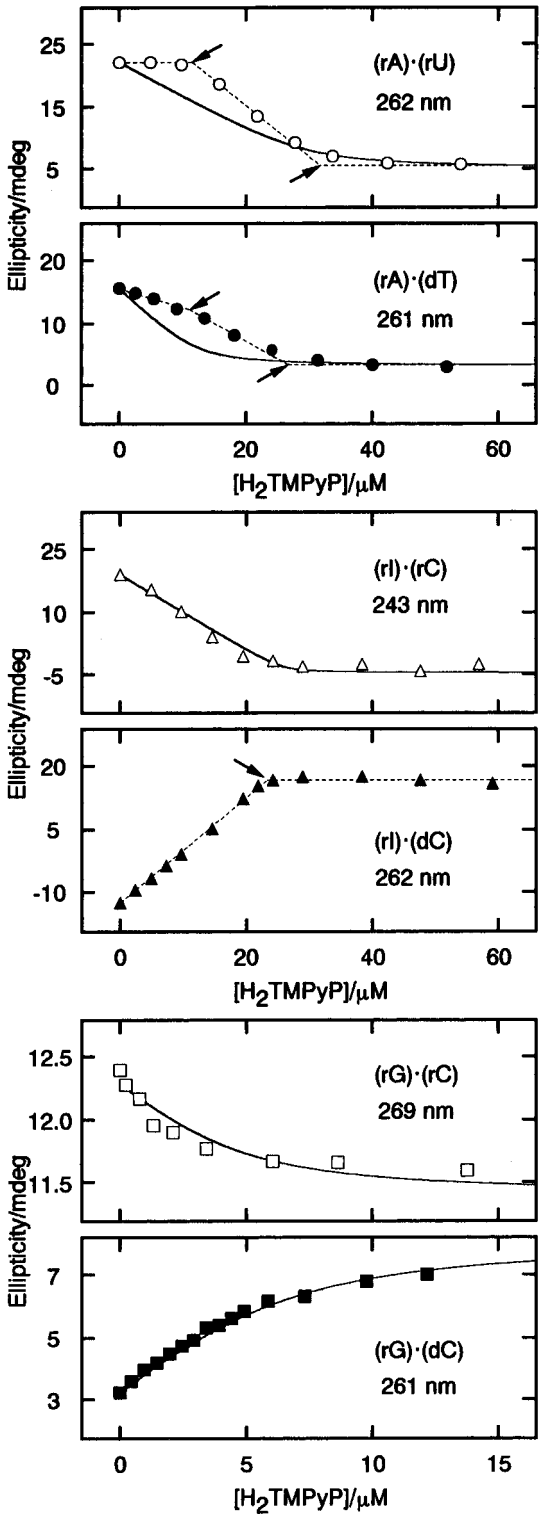

Figure 7. Changes in ellipticity of the duplexes upon addition of H_2TMPyP. The nucleotide concentrations were given in Figures 5 and 6. Key: Open circles, poly(rA)·poly(rU) at 262 nm; closed circles, poly(rA)·poly(dT) at 261 nm; open triangles, poly(rI)·poly(rC) at 243 nm; closed triangles, poly(rI)·poly(dC) at 262 nm; open squares, poly(rG)·poly(rC) at 269 nm; closed squares, poly(rG)·poly(dC) at 261 nm. The solid lines were drawn with the K and n_{AB} values in Table 2. The dashed lines were drawn with the linear part of the elliptic changes. The break points were marked with arrows.

For poly(rA)·poly(dT), two binding steps were detected by the elliptic change (Figure 7), and hence, we measured the induced CD spectrum with low duplex load corresponding to the $n = 0.7$ step. In the spectrum, however, only a weak negative peak was detected with low quality, and we could not identify the

Table 2. Binding Parameters of H_2TMPyP to the Duplexes

duplexes	$K/\mu M^{-1}$	n_{AB}[a]	n_{CD}[b]
poly(rA)·poly(rU)			0.30
	0.68	0.79	0.82
poly(rI)·poly(rC)	8.5	0.65	
poly(rG)·poly(rC)	0.73	0.11	
poly(rA)·poly(dT)	0.75	0.32	0.29
			0.69
poly(rI)·poly(dC)		0.25	
			0.59
		0.82	
poly(rG)·poly(dC)	0.55	0.15	
poly(dA-dT)$_2$[c]	1.2		
poly(dG-dC)$_2$[c]	0.77		

[a] The n values were obtained from the absorbance changes. [b] The n values were obtained from the elliptic changes. [c] From ref 46.

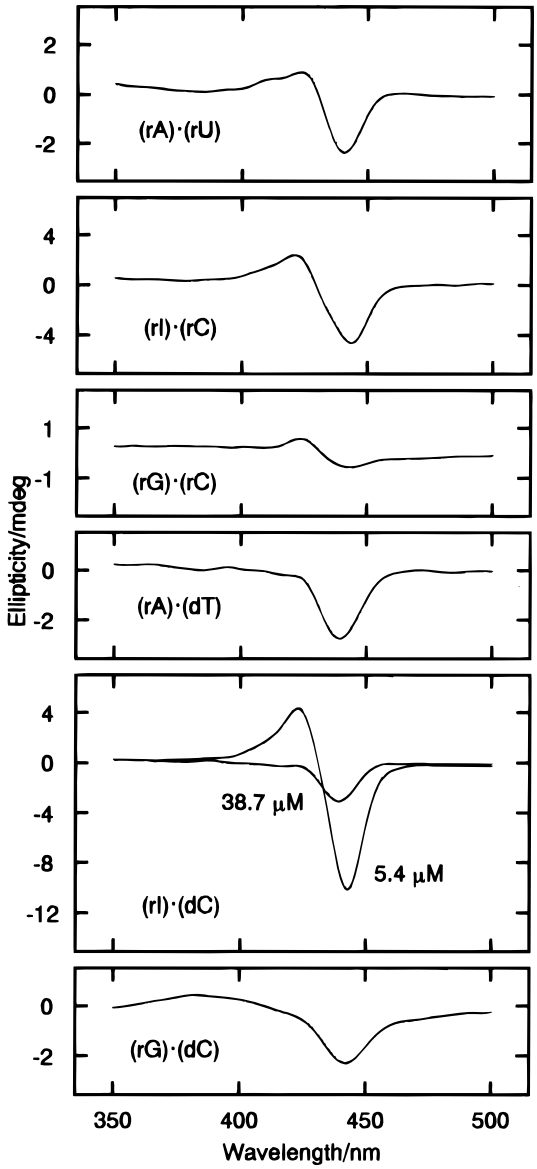

Figure 8. Induced CD spectra of H_2TMPyP by the addition of duplexes. The porphyrin concentration was 9.91 μM for poly(rG)·poly(rC) and 4.96 μM for the other duplexes. The spectra were recorded in 10 mM sodium phosphate, 1 mM EDTA, 0.1 M NaCl (pH 7.0). Key (from top to bottom): 31.2 μM poly(rA)·poly(rU); 27.9 μM poly(rI)·poly(rC); 237 μM poly(rG)·poly(rC); 58.8 μM poly(rA)·poly(dT); 5.4 and 38.7 μM poly(rI)·poly(dC); 255 μM poly(rG)·poly(dC).

binding mode for this step. In the case of poly(rI)·poly(dC), multiple binding steps were detected by the absorption and CD spectral changes (Figures 4 and 7), and hence, we measured

the induced CD spectra with loading lower and higher amounts of the duplex (Figure 8). When the duplex concentration was low, strong conservative-type CD peaks were induced, whereas only a negative CD peak was observed upon increasing the porphyrin concentration. Therefore, it is now clear that there are at least two modes, self-stacking and intercalation of the porphyrins, for the binding to poly(rI)·poly(dC).

Discussion

IC and GC Pairs. The binding process of the water-soluble cationic porphyrin, H_2TMPyP, to the RNA duplexes and DNA·RNA hybrids was investigated by absorption and CD spectral changes, and the binding parameters, *K* and *n*, were evaluated (Table 2). The porphyrin was found to bind externally with self-stacking to the RNA duplexes, poly(rG)·poly(rC) and poly(rI)·poly(rC), in a single step, and the binding parameters were very different between these duplexes. The difference should be originated from the 2-amino group on the guanine ring (Figure 1), which is hydrogen bonding to the cytosine on the opposite strand. The carbonyl oxygen on the cytosine base would become more electronegative when the hydrogen bonding is lost in the IC base pair, and the cationic porphyrin would have favored the negative charge developed on the carbonyl oxygen. Alternatively, the 2-amino group on the guanine would force steric repulsion when the porphyrin approaches the carbonyl oxygen and would prevent porphyrin binding. In either way, the self-stacking of the porphyrin should occur at the minor groove side where the 2-amino group is located.

In the case of poly(rI)·poly(dC), at least two steps were observed for the binding. Although the binding constant could not be evaluated, it is clear that this duplex afforded a greater number of binding sites than poly(rG)·poly(dC) ($n = 0.15$), and self-stacking of the porphyrins, in addition to the intercalative binding, was strongly suggested by the induced CD spectra (Figure 8). In the $n = 0.25$ step were observed the large hypochromicity and large bathochromic shift (Figure 3) with a negative induced CD peak (Figure 8), and hence, intercalation is attributed to this binding step. In the $n = 0.59$ step, which was detected by CD spectral change (Figure 7), the duplex conformation changed monotonously as it did in the $n = 0.25$ step, the porphyrin electronic structure being unchanged. At present, we are unable to assign the binding mode for this step, but partial intercalation[37,38] is one of the possible modes, since the porphyrin electrons should be perturbed similarly as they were in the intercalative $n = 0.25$ step. In the $n = 0.82$ step, the duplex conformation remain unchanged but the porphyrins should bind with self-stacking, as revealed by the induced CD spectrum (Figure 8). The partially intercalated porphyrins would be pulled out in this step to be stacked along the poly(rI)·poly(dC) surface.

AT and AU Pairs. A two-step process was observed in the case of poly(rA)·poly(rU) and poly(rA)·poly(dT) (Table 2). The first step with $n = 0.3$ for the poly(rA)·poly(rU) was only sensitive to the CD spectrum in the UV range, whereas the second $n = 0.8$ step was detected by both of the absorption and CD spectra. As we have revealed by the present study, the absorption spectrum was almost insensitive to the interchange of the binding modes between intercalation and the self-stacking. Therefore, the missing of the $n = 0.3$ step should suggest that either (or both) of these modes was responsible for this binding step. The induced CD spectrum was measured with a high poly(rA)·poly(rU) load relative to the porphyrin, and hence the spectrum should reflect the binding mode at the $n = 0.3$ step. Therefore, the remaining $n = 0.8$ step would be attributed mainly to the intercalation, which should perturb the porphyrin π electrons by the overlapping with the π electrons on the nucleobases.

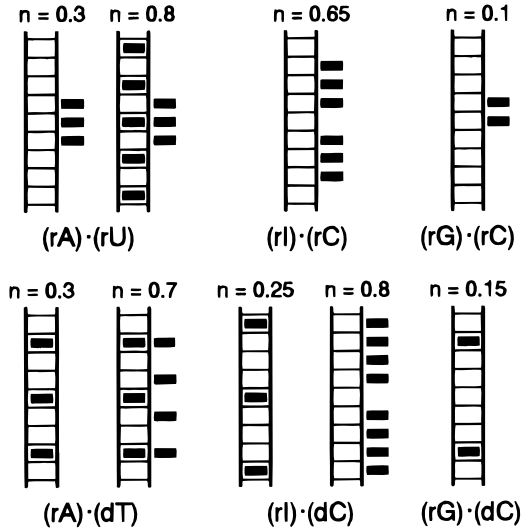

Figure 9. Schematic drawing of the binding mode of H_2TMPyP to the duplexes. The black squares represent the porphyrin, and the ladders indicate the duplexes.

The $n = 0.3$ step was detected in the other duplex poly(rA)·poly(dT) by both absorbance and CD studies (Table 2). The negative induced CD peak (Figure 7), along with the large bathochromic shift and hypochromicity (Table 1), strongly suggested the intercalative binding (Figure 9). The bathochromic shift and hypochromicity (Table 1), as well as the binding constant (Table 2), are comparable with those reported in the intercalative binding of H_2TMPyP with poly(dG-dC)$_2$.[46] The $n = 0.7$ step was not detected by absorbance change, indicating that the porphyrin π system was almost unaffected in this binding step. The large *n* value may suggest considerable interaction among the bound porphyrins and that self-stacking would be possible. If so, however, large conservative-type CD signals should be induced, which was not the case. Therefore, the $n = 0.7$ binding step may involve the external groove binding (Figure 9). When the intercalation occurred in the $n = 0.3$ step, the adjacent base pairs should be separated further by about 0.34 nm and the periodic nature of the sugar−phosphate backbone will be perturbed.[64] Therefore, the regular alignment of the porphyrin upon groove binding will be perturbed and the expected positive CD band might not be induced in the $n = 0.7$ step.

Induced CD. In the case of poly(rI)·poly(dC), two binding modes were apparent, but the absorption spectra seemed to have isosbestic points (Figure 3). Therefore, the absorption spectroscopy was unable to distinguish intercalation from self-stacking of the porphyrin. On the contrary, the induced CD spectroscopy was very powerful to reveal the binding mode of the porphyrin, as noted earlier.[46,56] We have summarized the intensity of the bisignate-induced CD peaks, and the molar ellipticity was found to be proportional to the *n* value (Figure 10). Two linear lines were drawn with zero-intercept for the positive bands at about 420 nm and the negative bands at about 440 nm, respectively. The larger *n* value indicates that the porphyrins are binding more densely to a duplex, and hence, the proportionality suggests that the transition moments of the porphyrin are aligned regularly upon binding of more and more porphyrin molecules, which resulted in the strong induced CD peaks. This corresponds to the previous observation[16] that the

(64) Berman, H. M.; Stallings, W.; Carrell, H. L.; Glusker, J. P.; Neidle, S.; Taylor, G.; Achari, A. *Biopolymers* **1979**, *18*, 2405−2429.

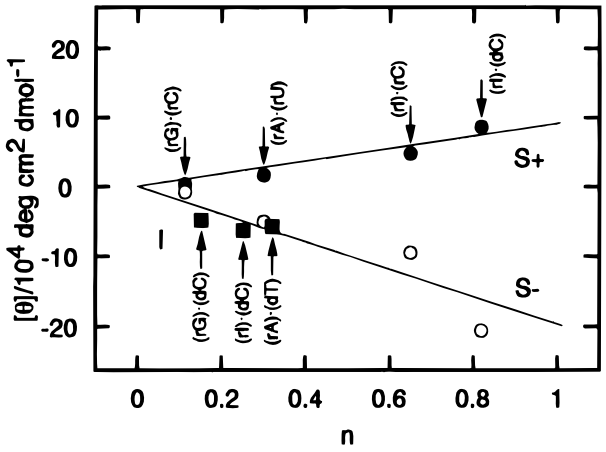

Figure 10. Correlations between the number of binding sites (*n*) and the molar ellipticities of the porphyrin-induced CD peaks. Two lines for the positive bands at about 420 nm and the negative bands at about 440 nm were drawn with zero-intercept. Key: Open circles, negative bands for self-stacking (S−); closed circles, positive bands for self-stacking (S+); closed squares, negative bands for intercalation (I).

self-assembly of porphyrins was induced by the addition of salt to produce very large CD peaks.

The intensity of the negative peaks at about 440 nm for the intercalative binding was nearly constant, and the *n* values were limited to the range of 0.1−0.3. If the nearest-neighbor exclusion principle also applies to the intercalation to the hybrids, the porphyrins should be separated more than 1 nm[65] and the porphyrin transition moments would not interact considerably with each other.

Binding Modes. The binding modes for the six duplexes examined are shown schematically in Figure 9. For poly(rI)·poly(dC), the binding mode at the $n = 0.59$ step, which was detected only by the CD spectral change (Table 2), was not clear and is not shown. The final step with $n = 0.82$ should be self-stacking, but some amount of the porphyrin might be intercalating at this step. The negative CD peak at about 440 nm for the intercalative binding might be buried under the strong induced peak for the self-stacking (Figure 8). As shown in Figure 10, however, the positive component is located on the straight line, as is the negative one for poly(rI)·poly(dC), such that we tentatively assign this binding step to contain only the self-stacking mode. A further structural study is necessary to determine the binding mode unequivocally.

To see the binding scheme in Figure 9, along with the induced CD signals summarized in Table 1, it is now clear that, at least at the first binding stage, the self-stacking is preferred commonly for RNA duplexes, whereas intercalation is favored for DNA·RNA hybrids. These findings do not depend on the base composition but only on whether the polynucleotide contains ribose or deoxyribose. In RNA duplexes, the displacement of the base pairs from the helical axis is considerable, with the base plane tilted away from the plane vertical to the axis.[66] These features should prevent the porphyrin from being accommodated between the base planes; thus, intercalation of a large porphyrin molecule should be unfavored. For the groove binding, the minor groove becomes wider and shallower in the RNA duplex than that in a DNA duplex, and the phosphate groups locate closer.[66] The binding to the minor groove would neutralize the negative charge on the phosphates, and the groove is now wide enough to accommodate the self-stacked porphyrin molecules.

The conformation of hybrids has been suggested to be an A form.[67] In poly(rA)·poly(dT), however, the ribose on the poly(rA) strand contains a C3′-*endo* sugar pucker while poly(dT) strand contains a C2′-*endo* pucker, which disturbs the symmetric property.[68] The C3′-*endo* pucker is favored by the intercalation, since the conformation is unchanged by this binding mode.[69] Although the conformation of the poly(rI)·poly(dC) and poly(rG)·poly(dC) has been claimed[70] to be an A form as in RNA duplexes, we propose here that the deoxyribonucleotides may readily change their conformation to a C2′-*endo* pucker. It should be noted that the conformation of poly(rA)·poly(dT) was once proposed to be an A form, which turned out to be a true hybrid containing C3′-*endo* riboses and C2′-*endo* deoxyriboses on the respective strands.[71,72] In any case, the pattern of the induced CD spectrum would be very sensitive to the conformation of the nucleotide polymers.

Conclusion

The binding properties of H_2TMPyP to RNA and DNA·RNA hybrid duplexes were studied by absorption and CD spectroscopic techniques. The predominant binding modes for RNA and hybrid duplexes were suggested to be self-stacking and intercalation, respectively. The molar ellipticity of the induced CD bands was found to be proportional to the number of the binding sites on the duplexes. Considerable interactions between the transition moments on the porphyrin, and hence the close contact of the porphyrins, were suggested. The present results afford ways to control the binding mode of a porphyrin drug to a nucleotide and to evaluate the binding modes.

Acknowledgment. This work was supported in part by a Grant-in-Aid (Nos. 04771907, 06772104, and 08672478 to T.U.) from the Ministry of Education, Science, and Culture of Japan.

IC960824A

(65) Arnott, S.; Bond, P. J.; Chandrasekaran, R. *Nature* **1980**, *287*, 561−563.
(66) Saenger, W. *Principles of Nucleic Acid Structure*; Springer Verlag: New York, 1984; Section 9.2.
(67) Milman, G.; Langridge, R.; Chamberlin, M. J. *Proc. Natl. Acad. Sci. U.S.A.* **1967**, *57*, 1804−1810.
(68) Zimmerman, S. B.; Pheiffer, B. H. *Proc. Natl. Acad. Sci. U.S.A.* **1981**, *78*, 78−82.
(69) Alden, C. J.; Arnott, S. *Nucleic Acids Res.* **1975**, *2*, 1701−1717.
(70) O'Brien, E. J.; MacEwan, A. W. *J. Mol. Biol.* **1970**, *48*, 243−261.
(71) Benevides, J. M.; Thomas, G. J., Jr. *Biochemistry* **1988**, *27*, 3868−3873.
(72) Arnott, S.; Chandrasekaran, R.; Hall, I. H.; Puigjaner, L. C. *Nucleic Acids Res.* **1983**, *11*, 4141−4155.